coatings

MDPI

Article

$ZnO_{np}/CaCO_3$ Core–Shell Nanoparticle Coatings on Kraft Paper: A Comparative Study of Antimicrobial Efficacy, Tensile Strength, and Hydrophobicity

Theerarat Sengsuk [1], Nicha Yotthanon [1], Ponusa Songtipya [1,2], Yeampon Nakaramontri [3], Waranyou Sridach [1,2] and Ladawan Songtipya [1,2,*]

[1] Packaging and Materials Technology Program, Faculty of Agro-Industry, Prince of Songkla University, Hat-Yai 90110, Songkhla, Thailand; theerarat.s@psu.ac.th (T.S.); nicha.y@psu.ac.th (N.Y.); ponusa.s@psu.ac.th (P.S.); waranyou.s@psu.ac.th (W.S.)
[2] Center of Excellence in Bio-Based Materials and Packaging Innovation, Prince of Songkla University, Hat-Yai 90110, Songkhla, Thailand
[3] Sustainable Polymer & Innovative Composite Materials Research Group, Department of Chemistry, King Mongkut's University of Technology Thonburi, Bangkok 10140, Thailand; yeampon.nak@kmutt.ac.th
* Correspondence: ladawan.so@psu.ac.th

Abstract: This study introduces a novel paper coating approach using modified zinc oxide (ZnO), providing a comparison with conventional materials used in the paper industry. The research focused on determining the concentration for effective microbial growth inhibition and evaluates the impact of different ZnO types on coated-paper properties, including antimicrobial activity, surface morphology, tensile strength, and water absorption. Specifically, ZnO microparticles (ZnO_{ws}), ZnO nanoparticles (ZnO_{np}), and modified ZnO_{np} (ZnO_{np}-$CaCO_3$, with a core–shell structure composed of calcium carbonate [$CaCO_3$] and nano-zinc oxide) were incorporated into coating formulations at varying concentrations (0 × MIC, 1 × MIC, 2 × MIC, and 3 × MIC, based on minimum inhibitory concentrations [MICs]). The results demonstrated that among all tested microorganisms, ZnO_{np}-$CaCO_3$ showed the lowest MIC values. ZnO_{np}-$CaCO_3$-coated paper exhibited superior antimicrobial activity against both Gram-positive and Gram-negative bacteria, as well as fungi, outperforming ZnO_{ws} and ZnO_{np}. At 1 × MIC, %inhibition for *E. coli*, *S. aureus*, and *A. niger* were 98.3%, 99.1%, and 90.8%, respectively. Additionally, ZnO_{np}-$CaCO_3$ coatings caused minimal color change in the paper compared to the other ZnO variants. The coating did not negatively impact the mechanical properties of the paper across all ZnO types and concentrations. Water absorption tests showed increased hydrophobicity with higher ZnO content, with ZnO_{np} and ZnO_{np}-$CaCO_3$ exhibiting greater reductions in water absorption than ZnO_{ws}. Overall, ZnO_{np}-$CaCO_3$ showed strong potential as an antimicrobial agent for paper surfaces, making it ideal for packaging and hygiene products. By partially replacing ZnO_{np} with inexpensive $CaCO_3$ core particles, ZnO_{np}-$CaCO_3$ delivers enhanced performance, reduced costs, and greater sustainability for large-scale applications.

Keywords: kraft paper; coating; zinc oxide nanoparticles; $CaCO_3$; antimicrobial

check for updates

Citation: Sengsuk, T.; Yotthanon, N.; Songtipya, P.; Nakaramontri, Y.; Sridach, W.; Songtipya, L. $ZnO_{np}/CaCO_3$ Core–Shell Nanoparticle Coatings on Kraft Paper: A Comparative Study of Antimicrobial Efficacy, Tensile Strength, and Hydrophobicity. *Coatings* **2024**, *14*, 1501. https://doi.org/10.3390/coatings14121501

Academic Editors: Apoorva Kulkarni and Kosuke Yoshinaga

Received: 31 October 2024
Revised: 22 November 2024
Accepted: 27 November 2024
Published: 28 November 2024

Copyright: © 2024 by the authors. Licensee MDPI, Basel, Switzerland. This article is an open access article distributed under the terms and conditions of the Creative Commons Attribution (CC BY) license (https://creativecommons.org/licenses/by/4.0/).

1. Introduction

Zinc oxide nanoparticles (ZnO_{np}) are produced synthetically and typically have sizes ranging from a few to one hundred nanometers. They exhibit unique properties, such as photocatalytic activity, semiconductor properties, and UV absorption [1–3]. Moreover, as indicated by numerous studies, they possess inherent antibacterial properties against several types of microorganisms, including (i) Gram-positive bacteria, such as *Staphylococcus aureus* (*S. aureus*), *Listeria monocytogenes*, and *Bacillus subtilis* [4–6]; (ii) Gram-negative bacteria, such as *Escherichia coli* (*E. coli*) [4] and *Pseudomonas aeruginosa* [4,5]; (iii) viruses, such as the influenza virus [7]; and (iv) fungi, including, for example, *Candida albicans*, *Aspergillus flavus*,

and *Aspergillus niger* [5–9]. However, Gram-negative bacteria commonly exhibit greater sensitivity to ZnO_{np} than Gram-positive bacteria due to the structure and composition of their cell walls [4]. The antimicrobial activity of ZnO_{np} is mainly attributed to the release of zinc ions (Zn^{2+}) and the generation of reactive oxygen species (ROS) [4,10–12]; Zn^{2+} play a crucial role in disrupting bacterial cell membranes and interfering with cellular processes, and ROS, such as superoxide radicals and hydrogen peroxide, can induce oxidative stress, leading to damage to bacterial DNA, proteins, and cell membranes [4,11]. Compared to micronized zinc oxide, ZnO_{np} has a larger specific surface area to enhance particle surface reactivity, resulting in more efficient antimicrobial inhibition [13,14].

Using ZnO_{np} in paper coatings has recently gained considerable attention because of the cost efficiency, outstanding antimicrobial activities [4–9], and UV absorption [1–3] of these nanoparticles. As evident from previous research, adding ZnO_{np} to coating agents is a promising route for enhancing various properties of paper, including its optical characteristics [15–17], mechanical properties [15,17], water resistance [16,17], and antimicrobial efficiency [15,17]. ZnO_{np} is generally white; therefore, it usually enhances the whiteness and brightness of coated papers, especially at higher concentrations [16,18]. Moreover, previous studies have shown that applying ZnO_{np} as a coating on bleached paper enhances its mechanical strength, with the improvement being proportional to the amount of ZnO_{np} used. For instance, Jia et al. reported that the tensile strength of coated paper in the machine direction increased from approximately 2.8 to 3.4 kN/m as the ZnO_{np} concentration in the coating agent increased from 0.1 to 0.2 g/100 mL [15]. This enhancement is likely attributable to the additional coating layer, which contains bonding substances and ZnO_{np} that act as reinforcing agents within the polymer matrix, collectively contributing to the increase in the overall strength of the paper. According to previous reports, ZnO_{np} also shows promise as an antimicrobial agent for paper coatings, making it applicable in hygiene-sensitive industries (e.g., biomedical applications and food packaging) [19]. Ghule et al. found that ZnO_{np}-coated paper successfully inhibited the growth of *E. coli*, even in the absence of light, with the bacterial count decreasing from 2.0×10^4 to 3.2×10^2 CFU after 1 h. Nevertheless, the antibacterial activity increased when the coated papers were illuminated with UV light (365 and 543 nm) with an increased exposure time [20]. In addition, Afsharpour and Imani recently investigated the antimicrobial activity of ZnO_{np}-coated paper against fungi (*A. niger* and *C. albicans*) and bacteria (*S. aureus* and *E. coli*) under visible light, with the coated paper samples exhibiting 100% inhibition of *S. aureus* and *E. coli* growth after 24 h. On the other hand, lower antimicrobial activity was observed for *A. niger* (>90% inhibition) and *C. albicans* (50% inhibition) after the same period [21].

However, according to thermodynamic theory, ZnO_{np} has a natural tendency to agglomerate, limiting its reactivity by reducing the surface free energy [22–24]. In this regard, previous studies have focused on enhancing the dispersion of ZnO_{np} by modifying the particles to form a core–shell structure; for example, ZnO_{np} has been coated on inorganic substances such as SiO_2, CaO, and $CaCO_3$ [25–27]. All research efforts have revealed a similar pattern of results: modifying ZnO_{np} could improve several of its surface properties, including its dispersion, enhancing its compatibility with polymer matrices. Furthermore, studies have shown that ZnO_{np} modified with $CaCO_3$ exhibits higher efficiency in the growth inhibition of microorganisms compared to normal ZnO_{np} when incorporated into natural rubber films [28]. However, no comparative studies have been conducted on the minimum amount of the substance needed to inhibit microbial growth and the application of such active substances as paper coating agents. Therefore, our research group aimed to investigate the development of antimicrobial paper using the core–shell structure of $CaCO_3$/nano-zinc oxide (ZnO_{np}-$CaCO_3$).

The main objective of this study was to investigate the minimum inhibitory concentration (MIC) of white seal ZnO (ZnO_{ws}), ZnO_{np}, and ZnO_{np}-$CaCO_3$ for the growth inhibition of Gram-positive and Gram-negative bacteria and fungi to compare their effectiveness and estimate the optimal ZnO concentration to use in a coating agent (cassava starch). Addi-

tionally, the study aimed to examine the influence of the ZnO coatings on the appearance, morphology, tensile strength, and water absorption of kraft paper.

2. Materials and Methods

2.1. Materials

Kraft paper (unbleached paper) with a basis weight of 320 g/m^2 was purchased from I Boom Co., Ltd., Bangkok, Thailand. Cassava starch (food-grade; Kriangkrai Co., Ltd., Bangkok, Thailand) was used as a polymer matrix to prepare the coating solutions. ZnO_{ws} (99.0% purity) was purchased from Kemaus, Elago Enterprises Pty Ltd., Sydney, Australia. Commercial-grade ZnO_{np} (97.8% purity) and modified ZnO_{np} (ZnO_{np}-$CaCO_3$, with a ZnO_{np}:$CaCO_3$ weight ratio of 90:10, 91.4% purity) were supplied by Global Chemical Co., Ltd., Samutprakarn, Thailand. Nutrient agar (NA), potato dextrose agar (PDA), nutrient broth (NB), and potato dextrose broth (PDB) were sourced from HiMedia Laboratories Pvt. Ltd., Mumbai, India, and were employed in the microbial cultures. Glutaraldehyde (25.0% purity, AR-grade; Loba Chemie Pvt. Ltd., Mumbai, India) was used as a fixing agent for the scanning electron microscopy (SEM) microbial samples, while anhydrous ethyl alcohol (99.9% purity, AR-grade; Daejung Chemical & Metals Co., Ltd., Siheung, Republic of Korea) was utilized as a dehydrating agent.

2.2. Preparation of Stock Solutions of Bacteria and Fungi

E. coli and *S. aureus* bacterial cultures were purified using a streak plate technique on NA and incubated at 37 °C for 24 h. Subsequently, isolated colonies were cultivated in NB and incubated under the same conditions to yield purified cultures. The fungus *A. niger* was purified via streaking on PDA and subsequent incubation at 37 °C for 72 h. The fungal spores from a single colony were inoculated into PDB and incubated at 37 °C for 72 h.

Stock solutions were prepared after cell purification, and the broth cultures of all microorganisms were diluted using their NB culture media to achieve a concentration of 1.5×10^8 CFU/mL, aligned with a 0.5 McFarland turbidity standard; their optical density at 600 nm (OD_{600}) was also determined using a spectrophotometer (UV-1800 Shimadzu, Kyoto, Japan).

2.3. Minimum Inhibitory Concentration (MIC) Determination

The MIC represents the lowest concentration of a substance capable of inhibiting microbial growth within a specified time. In this study, we assessed the MICs of various types of ZnO, including ZnO_{ws}, ZnO_{np}, and ZnO_{np}-$CaCO_3$, to determine their antimicrobial activity against both Gram-positive (*S. aureus*) and Gram-negative (*E. coli*) bacteria and fungi (*A. niger*). Aqueous dispersions of ZnO (25.0 wt%) were prepared via a ball-milling technique using 15 mm silicate balls over 7 days before conducting the experiments.

The MIC values of the ZnO samples were determined using a broth dilution method modified from the method of Little et al. [29]. *E. coli* and *S. aureus* stock cultures were appropriately diluted with NB to yield a concentration of 10^6 CFU/mL. Each type of ZnO was introduced into the broth cultures at varying concentrations within the range of 0–320 mg/mL, followed by incubation at 37 °C for 24 h. The MIC was determined as the lowest concentration with no observable visual turbidity, as shown in Figure 1.

In the case of *A. niger*, the culture broth was also diluted with PDB to achieve a concentration of 10^6 CFU/mL. Subsequently, MIC testing was performed following a similar procedure to that for the bacterial samples, applying an incubation temperature and time of 37 °C and 72 h, respectively. The MIC was determined by observing the tubes in which the fungi did not exhibit growth, that is, those without mycelium development or spore formation (Figure 1).

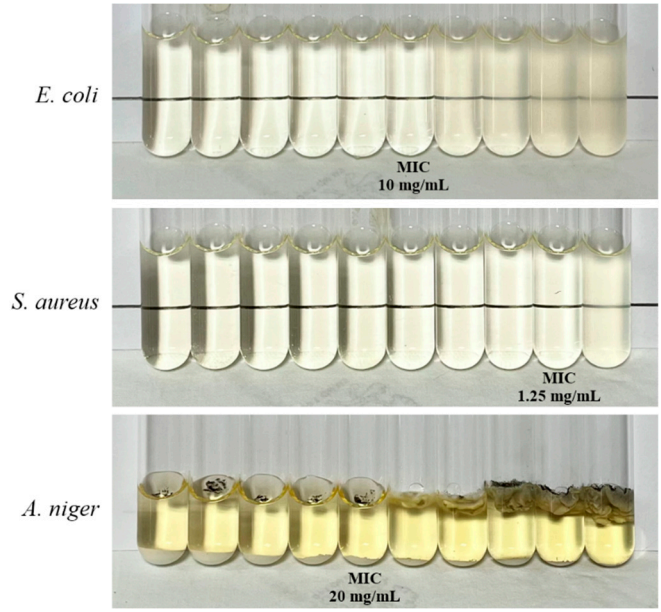


Figure 1. MIC testing of the effect of ZnO_{np}-$CaCO_3$ on the growth of *E. coli*, *S. aureus*, and *A. niger.*

2.4. Paper Coating

A cassava starch solution (3 wt%) was used as the coating agent. The starch powder was weighed and slowly added to distilled water. The starch was gelatinized at 90 °C for 30 min with continuous stirring, and ball-milled ZnO dispersions were added to the starch solution at different concentrations: 0 × MIC, 1 × MIC, 2 × MIC, and 3 × MIC. The mixtures were homogenized using a homogenizer (T25 digital Ultra Turrax, IKA, Staufen, Germany) at a rotational speed of 300 rpm for 30 min. The mixtures were sonicated for an additional 30 min [29] before being applied to kraft paper using a bar-coating applicator (AB4120, TQC Sheen, Zwijndrecht, Netherlands) equipped with a stainless-steel wire-wound applicator rod (AB3057) at a coating speed of 10 mm/s. The coating conditions (quantity of coating agent) were adjusted to achieve the desired coating weight of 16 ± 0.23 g/m^2. The coated paper was subsequently dried in a hot-air oven at 90 °C for 10 min [30].

2.5. Color Measurements

The coated paper samples were cut into 3 × 3 cm^2 pieces and placed on the measurement area of a colorimeter (ColorFle, HunterLab, Reston, VA, USA), according to the ASTM E1347 test method, to obtain the L* (lightness), a* (red/green coordinate), b* (yellow/blue coordinate) and ΔE* (the color difference) values. The reported ΔE* value was obtained by comparing the color values of the paper samples with those of a white standard paper used for color testing. A lower ΔE* value indicates greater whiteness of the paper, while a higher value suggests less whiteness.

2.6. Surface Morphology of Coated Papers

The coated papers were cut into small pieces, approximately 1 × 1 cm^2 in size, and placed on a stub. The sample surfaces were coated with gold, and the surface morphologies were examined via SEM (SU3900, Hitachi, Tokyo, Japan).

2.7. Growth Inhibition of Coated Papers

The stock cultures of *E. coli* and *S. aureus* were diluted with NB to achieve a bacterial concentration of 10^6 CFU/mL, and 5 mL aliquots of these diluted cultures were added to test tubes. Each coated paper, with a total surface area of 9.0 cm^2, was divided into four 0.75 × 3.00 cm^2 pieces, which were placed into a test tube and incubated at 37 °C for 24 h. The cell cultures were subsequently diluted to obtain a stepwise series of dilutions varying from 10^1 to 10^6 CFU/mL in concentration. The diluted cultures were then inoculated into NA

using the drop plate technique and incubated at 37 °C for 24 h. The bacterial colonies were counted, and the percentage growth inhibition was calculated according to Equation (1). Negative controls comprised untreated cell cultures, while positive controls involved cells cultured with ZnO.

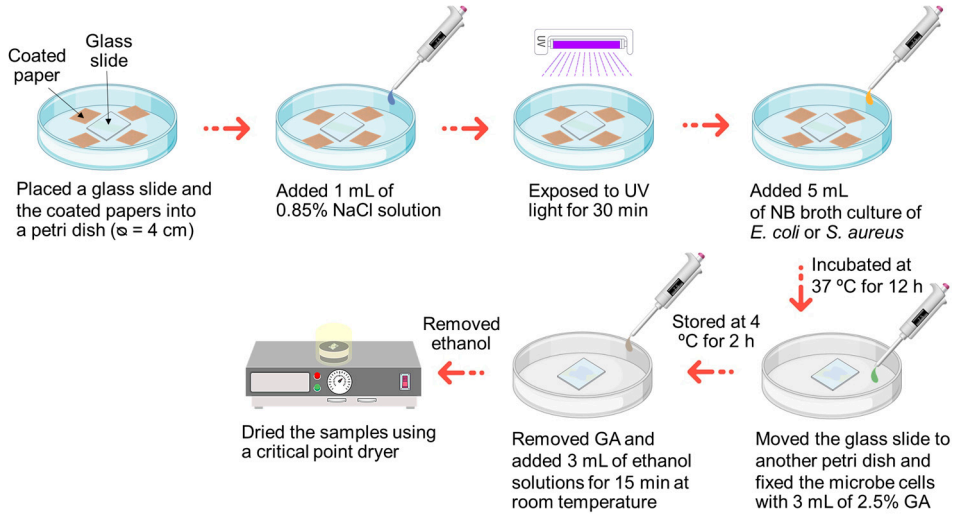
The *A. niger* culture was initially grown on PDA agar in a Petri dish at 37 °C for 72 h. Using a cork borer [31], the culture was circular-sectioned into 5.0 mm diameter pieces and transferred to a Petri dish containing the coated paper substrate, with PDB as the nutrient medium. The samples were then incubated at 37 °C for an additional 72 h. The fungal colony radius (the spread of the colony on the PDA surface) was measured [32], and the percentage of growth inhibition was calculated using Equation (1):

$$\% \text{ Growth Inhibition} = \frac{A - B}{A} \times 100 \quad (1)$$

where A is the initial number of bacterial colonies (CFU/mL) or initial fungal colony diameter (mm) before treatment and B is the final number of bacterial colonies (CFU/mL) or final fungal colony diameter (mm) after treatment.

2.8. Investigation of Microbe Morphology

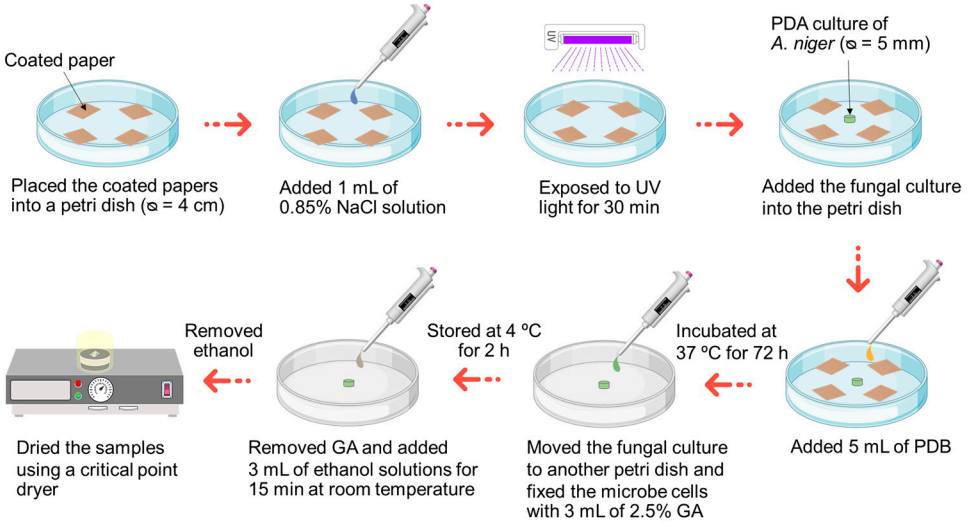
The sample preparation procedure for the SEM analysis of the tested bacteria was adapted from the methodology outlined by Kammoun et al. [33] and Yu et al. [34], as illustrated in Scheme 1. A glass slide (1 × 1 cm^2) and the coated papers (four pieces, each 1.5 × 1.5 cm^2 in size) were positioned in a cell culture dish (4 cm in diameter), ensuring that the coated side of the paper faced upwards. Subsequently, 1 mL of a 0.85% sodium chloride (NaCl) solution was added to the dish before UV exposure for 30 min. The 10^6 CFU/mL *E. coli* and *S. aureus* bacterial broth cultures (5 mL) were added to the dish, followed by incubation at 37 °C for 12 h. Thereafter, the glass slide was moved to another Petri dish, and the adherent bacteria on the slide were fixed using 3 mL of a 2.5% glutaraldehyde (GA) solution and stored at 4 °C for 2 h. The GA was then removed, and the samples were gradually dehydrated in a series of ethanol solutions (3 mL) of increasing concentration (25, 50, 80, 90, and 100%) for 15 min at ambient temperature, repeating each concentration twice. Finally, the ethanol was removed from the dish, and the samples were dried via critical point drying (CPD).



Scheme 1. Schematic diagram of the bacterial fixation procedure (*E. coli* and *S. aureus*) for morphological analysis via SEM.

The preparation of fungal samples (Scheme 2) also followed the modified methods of Kammoun et al. [33] and Yu et al. [34]. The coated papers were placed in a Petri dish, followed by the addition of 1 mL of a 0.85% NaCl solution and exposure to UV light for

30 min. The *A. niger* microbial culture was initially cultivated on PDA agar in a Petri dish at 37 °C for 72 h. The culture was then sectioned into 5.0 mm diameter pieces using a cork borer [31] and transferred to a Petri dish containing a coated paper substrate. Five milliliters of PDB was then added, and the setup was incubated at 37 °C for another 72 h. Subsequently, the *A. niger* culture was transferred to another dish and fixed with a 2.5% GA solution (3 mL). The samples were then dehydrated using a series of ethanol solutions, similar to the procedure followed for the bacterial samples, before removing the ethanol and drying via CPD.



Scheme 2. Schematic diagram of the fungal fixation procedure (*A. niger*) for morphological analysis via SEM.

The dried samples of all microbes were mounted onto a sample stub, and a fine layer of gold (10–20 nm) was deposited onto the sample surfaces using a sputter coater. The microbial morphology was subsequently examined via SEM (SU3900, Hitachi, Japan). The experiment was conducted similarly with the control sample, using paper coated with starch solution without ZnO.

2.9. Mechanical Properties

2.9.1. Tensile Strength

The tensile properties of the coated papers were assessed using the ASTM D828 standard [35] and a tensometer (H10ks Tinius Olsen, Horsham, PA, USA). The coated paper samples in the machine direction (MD) were precisely cut to dimensions of 1.5 × 25.4 cm^2 and conditioned at 25 ± 1 °C and 50% relative humidity (RH) for 24 h before testing. The tensile strength of the samples was analyzed with a pulling rate of 25.4 mm/min and a 5000 N load cell.

2.9.2. Water Absorption Capacity

The water absorption capacity (WAC_{cobb}) of the prepared coated papers, commonly referred to as the Cobb test, was measured according to the TAPPI T441 standard. Test specimens, 14 × 14 cm^2 in size, were cut and conditioned at a temperature of 27 ± 1 °C and an RH of 65 ± 2%. The coated papers were subsequently weighed before conducting the test. The specimens were assembled in a Cobb sizing tester, and 100 mL of water was poured onto the paper surface for 2 min. The water was drained after the specified time, and the excess water on the paper surface was removed by placing blotting paper over it and applying a 10 kg metal roller. Finally, the test specimens were reweighed to determine the weight difference.

2.10. Statistical Analysis

Mean comparisons of the experimental results were conducted using Duncan's multiple-range test with SPSS® software version 22.0 (SPSS Inc., Chicago, IL, USA). The significance level for all statistical tests was set at $p \leq 0.05$.

3. Results and Discussion

3.1. Minimum Inhibitory Concentration (MIC) of ZnO Particles

Table 1 presents the MIC values for each type of ZnO against *E. coli*, *S. aureus*, and *A. niger*. ZnO_{np}-$CaCO_3$ exhibited the lowest MIC values across all tested microorganisms, indicating that it is more effective in inhibiting bacteria and fungi than the other two types of ZnO. This may be attributed to the reduction in the ZnO_{np} particle size after modification with $CaCO_3$ [28] (see Table 1), resulting in an increase in the surface area. This could enhance the interactions between ZnO_{np}-$CaCO_3$ and environmental factors, such as moisture and oxygen, leading to an elevated production of ROS via photocatalytic processes and the release of Zn^{2+} ions, resulting in the effective inhibition of microbial growth [28].

Table 1. Particle sizes and MIC values of different types of ZnO.

ZnO Types	Particle Sizes (nm) *	MIC (mg/mL)		
		E. coli	***S. aureus***	***A. niger***
ZnO_{ws}	7697	320	320	>320
ZnO_{np}	194	80	5	160
ZnO_{np}-$CaCO_3$	171	10	1.25	20

* The particle size (agglomerated cluster) data were obtained from our previous study [28].

ZnO_{np} and ZnO_{np}-$CaCO_3$ exhibited more effective growth inhibition of *S. aureus* compared to *E. coli*. A plausible explanation is that the inhibition level of each microbe typically depends on the sensitivity of the microorganisms, which possess different cell wall structures [36], and their ability to adapt to diverse environments for survival. A similar conclusion was drawn by Reddy et al. [37], who demonstrated that Gram-positive bacteria, such as *S. aureus*, are generally more susceptible to ZnO_{np} compared to Gram-negative bacteria, such as *E. coli*. The thicker peptidoglycan layer in Gram-positive bacteria facilitates ZnO attack, while Gram-negative bacteria contain lipopolysaccharides as an additional protective component. Therefore, higher ZnO concentrations might be required for inhibition against Gram-negative bacteria.

In the comparative analysis of antifungal and antibacterial efficiency, the ZnO compounds all showed higher MICs for the fungal species compared to the bacterial species, implying lower antimicrobial activity against the former. This finding was directly in line with the results reported by Pasquet et al. [38], who proposed that the antimicrobial efficiency of ZnO_{np} against fungi is lower than that against bacteria because fungi can adapt to a variety of conditions for survival. Fungi possess mechanisms to change their cellular structure, such as forming pores to facilitate gas exchange or releasing spores in challenging environments.

3.2. Properties of Coated Papers

3.2.1. Visual Appearance and Surface Morphology

Figure 2 illustrates the visual appearance (color characteristics) of the ZnO-coated papers; all ZnO types (ZnO_{ws}, ZnO_{np}, and ZnO_{np}-$CaCO_3$) contributed to a whitening effect of the paper surface. This observation aligned with the increase in L* values, especially when the ZnO concentration increased (Table 2), resulting in a reduction in the other color values of the kraft paper. This phenomenon can be attributed to the inherent whiteness of ZnO, which can scatter diverse wavelengths of light, enhancing the whiteness and

brightness of materials [15,16,39]. However, variations in the size and type of ZnO particles could lead to differential light scattering, consequently influencing the perceived color of the coated papers. Upon visual observation, ZnO_{np}-$CaCO_3$ exhibited the lowest degree of whiteness and opacity, particularly at a concentration of 3 × MIC. Based on this, it can be inferred that a smaller quantity of ZnO_{np}-$CaCO_3$ was required compared to other types of ZnO, owing to its lower minimum effective concentration for antimicrobial activity (see Table 1), resulting in the use of a smaller amount of the substance in coatings with the same MIC level. Furthermore, if compared at equivalent amounts of ZnO, the modified ZnO still contained fewer ZnO particles than the other types, particularly ZnO_{np}, due to the partial substitution by $CaCO_3$.

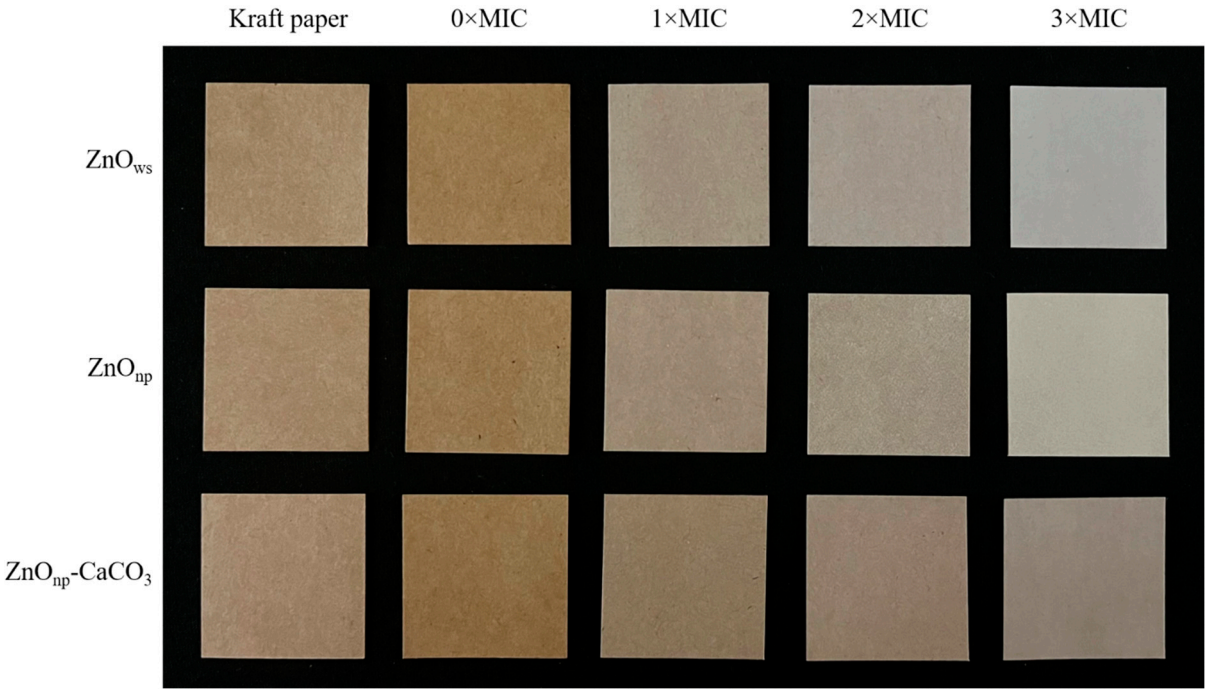


Figure 2. Visual appearance of the uncoated papers and the papers coated with different types and concentrations of ZnO.

Table 2. CIE L*, a*, b*, and ΔE* values of uncoated papers and papers coated with different types and concentrations of ZnO.

Samples		Color			
		L*	a*	b*	ΔE*
Uncoated		61.40 ± 0.34 ^{j}	7.74 ± 0.10 ^{b}	22.40 ± 0.21 ^{b}	39.35 ± 0.38 ^{b}
ZnO_{ws}	0 × MIC	58.39 ± 0.08 ^{k}	8.69 ± 0.08 ^{a}	26.44 ± 0.42 ^{a}	44.21 ± 0.16 ^{a}
	1 × MIC	68.96 ± 0.12 ^{e}	5.44 ± 0.06 ^{f}	7.72 ± 0.17 ^{h}	25.78 ± 0.10 ^{g}
	2 × MIC	74.48 ± 0.30 ^{c}	3.65 ± 0.15 ^{h}	4.63 ± 0.29 ^{i}	19.42 ± 0.36 ^{i}
	3 × MIC	78.78 ± 0.13 ^{b}	1.85 ± 0.07 ^{i}	3.56 ± 0.17 ^{j}	14.69 ± 0.13 ^{k}
ZnO_{np}	0 × MIC	58.39 ± 0.08 ^{k}	8.69 ± 0.08 ^{a}	26.44 ± 0.42 ^{a}	44.21 ± 0.16 ^{a}
	1 × MIC	65.48 ± 0.27 ^{h}	6.18 ± 0.16 ^{d}	15.52 ± 0.36 ^{d}	32.27 ± 0.15 ^{d}
	2 × MIC	66.21 ± 0.23 ^{g}	5.80 ± 0.01 ^{e}	14.43 ± 0.20 ^{e}	30.85 ± 0.16 ^{e}
	3 × MIC	80.66 ± 0.28 ^{a}	0.75 ± 0.06 ^{j}	9.82 ± 0.07 ^{g}	15.49 ± 0.24 ^{j}
ZnO_{np}-$CaCO_3$	0 × MIC	58.39 ± 0.08 ^{k}	8.69 ± 0.08 ^{a}	26.44 ± 0.42 ^{a}	44.21 ± 0.16 ^{a}
	1 × MIC	63.34 ± 0.29 ^{i}	6.92 ± 0.07 ^{c}	16.38 ± 0.14 ^{c}	34.50 ± 0.37 ^{c}
	2 × MIC	67.48 ± 0.22 ^{f}	5.45 ± 0.11 ^{f}	11.67 ± 0.10 ^{f}	28.49 ± 0.24 ^{f}
	3 × MIC	70.63 ± 0.29 ^{d}	4.14 ± 0.15 ^{g}	10.13 ± 0.10 ^{g}	24.64 ± 0.49 ^{h}

Note: Significant differences ($p < 0.05$) were indicated by different superscript letters in the columns.

SEM images of the uncoated and ZnO-coated kraft paper are presented in Figure 3. Complex interwoven cellulosic fibrils can be observed in the uncoated paper (Figure 3A); in contrast, the surface of the paper coated with starch solution (Figure 3B) appeared smooth and showed no visible fiber entanglement. In the ZnO-coated papers, there was a noticeable deposition of ZnO particles on the paper surfaces (Figure 3C–E). Among the different ZnO types, ZnO_{np} showed the highest tendency to agglomerate; this was likely due to its small particle size and large surface area, leading to strong attractive (electrostatic and London dispersion) forces between the particles [40,41]. Conversely, ZnO_{np}-$CaCO_3$ displays enhanced dispersion and finer particle characteristics; this could be attributed to the modification of ZnO with $CaCO_3$, as a core–shell structure can reduce the interaction between individual particles, resulting in a decrease in particle agglomeration. Therefore, the obtained paper was expected to have a smoother surface than the other ZnO-coated papers.

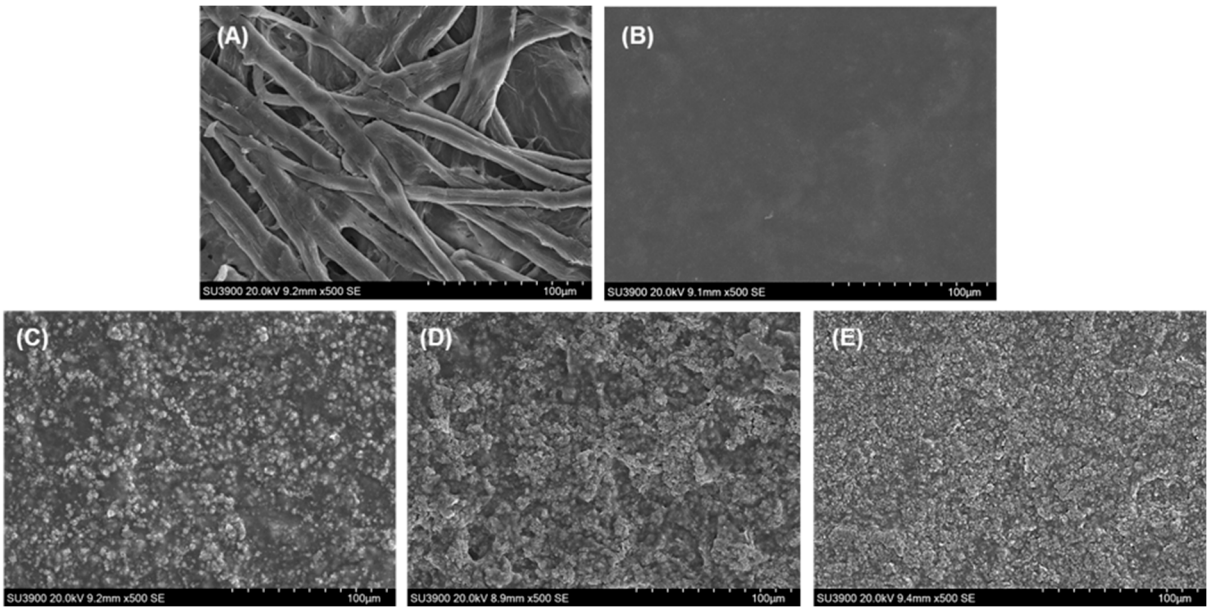


Figure 3. Surface images of (**A**) uncoated paper; (**B**) paper coated with a starch solution, without ZnO; and papers coated with (**C**) ZnO_{ws}, (**D**) ZnO_{np}, and (**E**) ZnO_{np}-$CaCO_3$ at 1 × MIC.

3.2.2. Microbial Growth Inhibition

The results revealed that the incorporation of ZnO_{np}-$CaCO_3$ into the coating material at a concentration of 1 × MIC effectively inhibited bacterial growth by ≥98% for *E. coli* and *S. aureus* (Figure 4A,B) and fungal growth by 90% for *A. niger* (Figure 4C). These inhibition values were higher than those for ZnO_{ws} at the same multiple levels of its own MIC. Moreover, when compared to ZnO_{np}, the modified ZnO demonstrated similar efficacy at the same MIC levels, except for *E. coli*, where its efficacy was slightly lower. Therefore, ZnO_{np}-$CaCO_3$ was the most effective and cost-efficient among the ZnO types.

The effects of ZnO_{np}-$CaCO_3$ on the cell morphology of *E. coli*, *S. aureus*, and *A. niger* were examined via SEM to confirm its antimicrobial properties, as illustrated in Figure 5. The untreated cells exhibited intact and smooth surfaces, while noticeable changes in the microbial morphologies occurred after treatment with the ZnO at 1 × MIC for 12 h, as expected. Uneven cell surfaces and irregular cell shapes implied a loss of membrane integrity, indicating bacterial and fungal cellular damage. A similar transformation in cell morphology has also been demonstrated in other metals or metal oxides, such as ZnO/Ag, Ag/Au, and MgO nanoparticles [42–44].

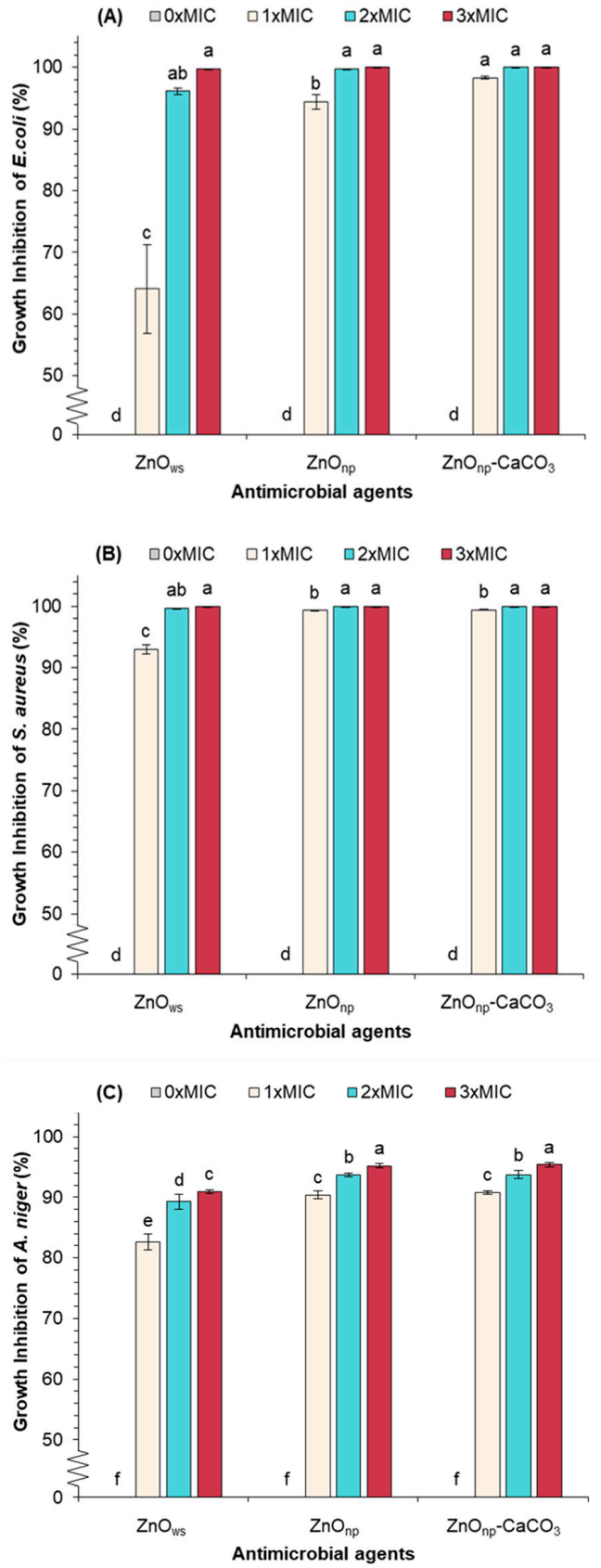


Figure 4. Growth inhibition of (**A**) *E. coli*, (**B**) *S. aureus*, and (**C**) *A. niger* by uncoated papers and papers coated with different types and concentrations of ZnO. Note: Significant differences ($p < 0.05$) were indicated by different letters above the bars.

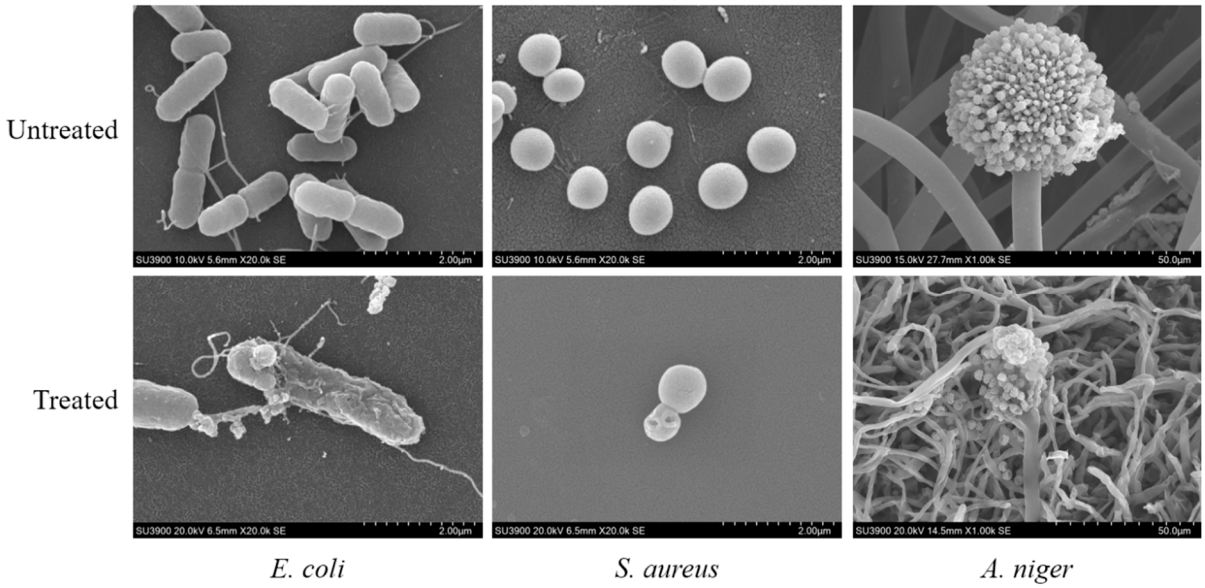


Figure 5. SEM images of fixed bacterial and fungal cells before and after treatment with 1 × MIC ZnO_{np}-$CaCO_3$.

3.2.3. Tensile Strength and Water Absorption

Table 3 presents the mechanical and water absorption properties of the uncoated and ZnO-coated papers. Based on the experimental results, it can be concluded that the tensile strength of the paper remains largely unchanged before (22.6 kN/m) and after coating (ranging from 20.6 to 23.5 kN/m). This suggested that the coating did not significantly affect the mechanical properties of the paper. However, the experimental results contrasted with those of Jia et al. [15], who coated bleached paper with ZnO_{np} and observed an increase in mechanical properties with higher ZnO_{np} concentrations. This discrepancy may be attributed to the role of ZnO_{np} as a reinforcing agent within the polymer matrix of the coating layer. When the coating itself is stronger than the paper substrate, it can contribute to an increase in the material's tensile strength. The differences in the type of paper (bleached vs. unbleached) and coating application may also play a significant role in the observed effects.

Table 3. Tensile strength and water absorption capacity (WAC_{cobb}) of uncoated and ZnO-coated papers.

Samples	ZnO Content	Tensile Strength (kN/m)	WAC_{cobb} (g/m^2)
Uncoated		22.57 ± 0.59 ^{ab}	58.33 ± 5.69 ^{ef}
ZnO_{ws}	0 × MIC	21.58 ± 0.38 ^{bcd}	93.00 ± 3.61 ^{a}
	1 × MIC	22.56 ± 1.14 ^{ab}	97.33 ± 2.52 ^{a}
	2 × MIC	22.85 ± 0.67 ^{ab}	70.67 ± 4.16 ^{d}
	3 × MIC	23.54 ± 1.25 ^{a}	73.00 ± 4.85 ^{cd}
ZnO_{np}	0 × MIC	21.58 ± 0.38 ^{bcd}	93.00 ± 3.61 ^{a}
	1 × MIC	20.63 ± 0.80 ^{cd}	85.33 ± 3.51 ^{b}
	2 × MIC	21.85 ± 0.66 ^{bcd}	55.33 ± 0.58 ^{ef}
	3 × MIC	22.86 ± 0.66 ^{ab}	57.67 ± 2.08 ^{ef}
ZnO_{np}-$CaCO_3$	0 × MIC	21.58 ± 0.38 ^{bcd}	93.00 ± 3.61 ^{a}
	1 × MIC	20.63 ± 0.68 ^{d}	78.33 ± 5.03 ^{c}
	2 × MIC	21.91 ± 0.46 ^{bc}	61.00 ± 5.57 ^{e}
	3 × MIC	22.50 ± 0.83 ^{ab}	51.67 ± 3.79 ^{f}

Note: Significant differences ($p < 0.05$) were indicated by different superscript letters in the columns.

The effect of the ZnO coatings on the water absorption properties of the paper was assessed via WAC_{cobb}. The starch-coated paper exhibited the highest WAC_{cobb}; this was attributable to the hydrophilic nature of starch, which is related to the presence of hydroxyl groups in its structure. However, the WAC_{cobb} tended to decrease with increasing ZnO content, suggesting that the ZnO types used in this study all displayed less hydrophilic behavior than starch. Therefore, increasing the quantity of ZnO led to increased hydrophobicity of the material surface; generally, even the surface of ZnO can exhibit hydrophobic or hydrophilic characteristics, depending on the physical and chemical properties of the ZnO [44]. Compared to the ZnO_{np}- and ZnO_{np}-$CaCO_3$-coated papers, the ZnO_{ws}-coated papers exhibited higher WAC_{cobb} values; this can be attributed to the larger ZnO_{ws} particle sizes (see Table 1) resulting in increased surface roughness of the coated paper and therefore a higher surface area and WAC_{cobb} [45,46]. Additionally, the larger ZnO_{ws} particles may be less effective in uniformly penetrating the paper surface compared to the smaller ZnO_{np} particles, which could have further contributed to the observed higher water absorption. However, coating the paper with ZnO_{np} and ZnO_{np}-$CaCO_3$ at concentrations of 2 × MIC and 3 × MIC (51.67–61.0 g/m^2) resulted in water absorption values comparable to those of the uncoated paper (58.33 g/m^2).

4. Conclusions

In conclusion, this study offers valuable insights into the effects of various ZnO coatings on the properties of paper. ZnO_{np}-$CaCO_3$ demonstrated effective antimicrobial properties, inhibiting bacterial and fungal growth with the lowest MIC value compared to ZnO_{ws} and ZnO_{np}. Coating the paper with 1 × MIC, ZnO_{np}-$CaCO_3$ inhibited the growth of Gram-positive/Gram-negative bacteria and a selected fungus by >98% and 90%, respectively, which was similar to ZnO_{np} at the same concentration, except for *E. coli*. Color changes and surface morphological variations highlighted the impact of ZnO on the appearance and surface structure of the coated papers. The whiteness of the coated papers increased significantly compared to the uncoated paper, depending on the ZnO concentration and type. In addition, the use of ZnO_{np}-$CaCO_3$ led to reduced agglomeration of the ZnO particles on the paper surface. Regarding the mechanical properties, the kraft paper showed no significant change in tensile strength for all ZnO types with increasing ZnO content. Furthermore, an increase in the hydrophobicity of the coated paper surface was observed for all ZnO types, suggesting the potential for customized water-resistant paper coatings; the ZnO_{np}-$CaCO_3$-coated sample (3 × MIC) exhibited the lowest water absorption. These findings contribute to elucidating the versatile properties of ZnO_{np}-$CaCO_3$-coated paper and the feasibility of using ZnO_{np}-$CaCO_3$ in paper technology. Nevertheless, further studies might be required to investigate the properties of coated papers fabricated from ZnO_{np}-$CaCO_3$ and coating materials other than cassava starch (exhibiting different polarity characteristics) to acquire materials with broader applicability.

Author Contributions: Investigation, T.S. and N.Y.; supervision, P.S. and W.S.; resources, Y.N.; conceptualization writing—original draft, writing—review and editing, visualization, supervision, project administration, L.S. All authors have read and agreed to the published version of the manuscript.

Funding: This research was supported by (i) the National Science, Research and Innovation Fund (NSRF) and (ii) the Prince of Songkla University, Thailand (Basic Research Fund: grant no. AGR6601352S). The authors thank the Global Chemical Co, Ltd., Thailand, for supplying the ZnO particles.

Institutional Review Board Statement: Ethical review and approval were waived for this study due to the study design not involving human or animal subjects.

Informed Consent Statement: Not applicable, as the study did not involve human participants.

Data Availability Statement: The data supporting the findings of this study are available from the corresponding author upon reasonable request. Due to privacy and ethical considerations, these data are not publicly accessible.

Conflicts of Interest: The authors confirm that no known competing financial interests or personal relationships might have influenced the work presented in this paper.

References

1. Chen, X.; Mao, S.S. Titanium dioxide nanomaterials: Synthesis, properties, modifications, and applications. *Chem. Rev.* **2007**, *107*, 2891–2959. [CrossRef] [PubMed]
2. Nayna, O.K.; Tareq, S.M. Application of Semiconductor Nanoparticles for Removal of Organic Pollutants or Dyes From Wastewater. In *Nanotechnology in Water and Wastewater Treatment*; Ahsan, A., Ismail, A.F., Eds.; Micro and Nano Technologies Series; Elsevier: Amsterdam, The Netherlands, 2019; pp. 267–290. [CrossRef]
3. Song, Z.; Kelf, T.A.; Sanchez, W.H.; Roberts, M.S.; Rička, J.; Frenz, M.; Zvyagin, A.V. Characterization of optical properties of ZnO nanoparticles for quantitative imaging of transdermal transport. *Biomed. Opt. Express* **2011**, *2*, 3321–3333. [CrossRef] [PubMed]
4. Mendes, C.R.; Dilarri, G.; Forsan, C.F.; Sapata, V.D.M.R.; Lopes, P.R.M.; de Moraes, P.B.; Montagnolli, R.N.; Ferreira, H.; Bidoia, E.D. Antibacterial action and target mechanisms of zinc oxide nanoparticles against bacterial pathogens. *Sci. Rep.* **2022**, *12*, 2658. [CrossRef] [PubMed]
5. Yagoub, A.E.A.; Al-Shammari, G.M.; Al-Harbi, L.N.; Subash-Babu, P.; Elsayim, R.; Mohammed, M.A.; Yahya, M.A.; Fattiny, S.Z.A. Antimicrobial properties of zinc oxide nanoparticles synthesized from Lavandula pubescens shoot methanol extract. *Appl. Sci.* **2022**, *12*, 11613. [CrossRef]
6. Mirhosseini, M.; Firouzabadi, F.B. Reduction of Listeria monocytogenes and Bacillus cereus in milk by zinc oxide nanoparticles. *Iran. J. Pathol.* **2015**, *10*, 97–104. [PubMed] [PubMed Central]
7. Ghaffari, H.; Tavakoli, A.; Moradi, A.; Tabarraei, A.; Bokharaei-Salim, F.; Zahmatkeshan, M.; Farahmand, M.; Javanmard, D.; Kiani, S.J.; Esghaei, M.; et al. Inhibition of H1N1 influenza virus infection by zinc oxide nanoparticles: Another emerging application of nanomedicine. *Biomed. Sci.* **2019**, *26*, 70. [CrossRef]
8. Hosseini, S.S.; Mohammadi, S.R.; Joshaghani, H.R.; Eskandari, M. Antifungal effect of sodium dodecyl sulfate and nanoparticle ZnO on growth inhibition of standard strain of *Candida albicans*. *Gorgan Univ. Med. Sci.* **2011**, *12*, 64–69.
9. Alhazmi, N.M.; Sharaf, E.M. Fungicidal activity of zinc oxide nanoparticles against azole-resistant *Aspergillus flavus* isolated from yellow and white maize. *Molecules* **2023**, *28*, 711. [CrossRef]
10. Hajipour, M.J.; Fromm, K.M.; Ashkarran, A.A.; de Aberasturi, D.J.; de Larramendi, I.R.; Rojo, T.; Serpooshan, V.; Parak, W.J.; Mahmoudi, M. Antibacterial properties of nanoparticles. *Trends Biotechnol.* **2012**, *30*, 499–511. [CrossRef]
11. Sirelkhatim, A.; Mahmud, S.; Seeni, A.; Kaus, N.H.M.; Ann, L.C.; Bakhori, S.K.M.; Hasan, H.; Mohamad, D. Review on zinc oxide nanoparticles: Antibacterial activity and toxicity mechanism. *J. Nano-Micro Lett.* **2015**, *7*, 219–242. [CrossRef]
12. Lallo da Silva, B.; Abuçafy, M.P.; Berbel Manaia, E.; Oshiro Junior, J.A.; Chiari-Andréo, B.G.; Pietro, R.C.R.; Chiavacci, L.A. Relationship between structure and antimicrobial activity of zinc oxide nanoparticles: An overview. *Int. J. Nanomedicine* **2019**, *14*, 9395–9410. [CrossRef] [PubMed]
13. Raghupathi, K.R.; Koodali, R.T.; Manna, A.C. Size-dependent bacterial growth inhibition and mechanism of antibacterial activity of zinc oxide nanoparticles. *Langmuir* **2011**, *27*, 4020–4028. [CrossRef] [PubMed]
14. Babayevska, N.; Przysiecka, Ł.; Iatsunskyi, I.; Nowaczyk, G.; Jarek, M.; Janiszewska, E.; Jurga, S. ZnO size and shape effect on antibacterial activity and cytotoxicity profile. *Sci. Rep.* **2022**, *17*, 8148. [CrossRef] [PubMed]
15. Jia, M.; Zhang, X.; Weng, J.; Zhang, J.; Zhang, M. Protective coating of paper works: ZnO/cellulose nanocrystal composites and analytical characterization. *Cult. Herit.* **2019**, *38*, 64–74. [CrossRef]
16. Prasad, V.; Shaikh, A.J.; Kathe, A.A.; Bisoyi, D.K.; Verma, A.K.; Vigneshwaran, N. Functional behavior of paper coated with zinc oxide–soluble starch nanocomposites. *J. Mater. Process Technol.* **2010**, *210*, 1962–1967. [CrossRef]
17. Ni, S.; Zhang, H.; Dai, H.; Xiao, H. Starch-based flexible coating for food packaging paper with exceptional hydrophobicity and antimicrobial activity. *Polymers* **2018**, *10*, 1260. [CrossRef]
18. Cheng, F.; Betts, J.W.; Kelly, S.M.; Wareham, D.W.; Kornherr, A.; Dumestre, F.; Schaller, J.; Heinze, T. Whiter, brighter and more stable cellulose paper coated with antibacterial carboxymethyl starch stabilized ZnO nanoparticles. *J. Mater. Chem. B* **2014**, *20*, 3057–3064. [CrossRef]
19. Espitia, P.J.P.; Otoni, C.G.; Soares, N.F.F. Chapter 34—Zinc oxide nanoparticles for food packaging applications. In *Antimicrobial Food Packaging*; Barros-Velázquez, J., Ed.; Academic Press: Cambridge, MA, USA, 2016; pp. 425–431. [CrossRef]
20. Ghule, K.; Ghule, A.V.; Chen, B.J.; Ling, Y.C. Preparation and characterization of ZnO nanoparticles coated paper and its antibacterial activity study. *Green Chem.* **2006**, *8*, 1034–1041. [CrossRef]
21. Afsharpour, M.; Imani, S. Preventive protection of paper works by using nanocomposite coating of zinc oxide. *Cult. Herit.* **2017**, *25*, 142–148. [CrossRef]
22. Roy, R.; Singh, S.K.; Chauhan, L.K.S.; Das, M.; Tripathi, A.; Dwivedi, P.D. Zinc oxide nanoparticles induce apoptosis by enhancement of autophagy via PI3K/Akt/mTOR inhibition. *Toxicol. Lett.* **2014**, *227*, 29–40. [CrossRef]
23. Hayeemasae, N.; Rathnayake, W.G.I.U.; Ismail, H. Effect of ZnO nanoparticles on the simultaneous improvement in curing and mechanical properties of NR/Recycled EPDM blends. *Prog. Rubber Plast. Recycl.* **2018**, *34*, 1–18. [CrossRef]
24. Hadi, F.A.; Kadhim, R.G. A study of the effect of nano zinc oxide on cure characteristics and mechanical properties of rubber composites. *J. Phys Conf. Ser.* **2019**, *1234*, 012043. [CrossRef]

25. Gaca, M.; Pietrasik, J.; Zaborski, M.; Okrasa, L.; Boiteux, G.; Gain, O.; Magdalena, G. Effect of zinc oxide modified silica particles on the molecular dynamics of carboxylated acrylonitrile-butadiene rubber composites. *Polymers* **2017**, *9*, 645. [CrossRef] [PubMed]
26. Wang, Z.; Hou, Z.; Liu, X.; Gu, Z.; Li, H.; Chen, Q. Preparation of zinc oxide with core–shell structure and its application in rubber products. *Polymers* **2023**, *15*, 2353. [CrossRef]
27. Gherekhlo, Z.D.; Motiee, F.; Khorrami, S. Synthesis of the CoO.CaO/ZnO core-shell nanopigment and investigation of its effects on the properties of rubber compounds based on the acrylonitrile butadiene elastomer (NBR). *IIOAB J.* **2016**, *7*, 394–400.
28. Krainoi, A.; Poomputsa, K.; Kalkornsurapranee, E.; Jobish, J.; Songtipya, L.; Nip, R.; Nakaramontri, Y. Disinfectant natural rubber films filled with modified zinc oxide nanoparticles: Synergetic effect of mechanical and antibacterial properties. *Express Polym. Lett.* **2021**, *15*, 1081–1110. [CrossRef]
29. Little, W.; Black, C.; Smith, A.C. Clinical implications of polymicrobial synergism effects on antimicrobial susceptibility. *Int. J. Pathogens.* **2021**, *10*, 144. [CrossRef]
30. Jung, J.; Raghavendra, G.M.; Kim, D.; Seo, J. One-step synthesis of starch-silver nanoparticle solution and its application to antibacterial paper coating. *Int. J. Biol. Macromol.* **2018**, *7*, 2285–2290. [CrossRef]
31. Paolino, B.; Sorrentino, M.C.; Troisi, J.; Delli Carri, M.; Kiselev, P.; Raimondo, R.; Lahoz, E.; Pacifico, S. Lavandula angustifolia Mill. for a suitable non-invasive treatment against fungal colonization on organic-media cultural heritage. *Herit. Sci.* **2024**, *12*, 53. [CrossRef]
32. Kamaruzzaman, M.; Islam, M.S.; Mahmud, S.; Polash, S.A.; Sultana, R.; Wang, C.; Jiang, C. In vitro and in silico approach of fungal growth inhibition by *Trichoderma asperellum* HbGT6-07 derived volatile organic compounds. *Arab. J. Chem.* **2021**, *14*, 103290. [CrossRef]
33. Kammoun, R.; Zmantar, T.; Ghoul, S. Scanning electron microscopy approach to observe bacterial adhesion to dental surfaces. *MethodsX.* **2020**, *7*, 101107. [CrossRef] [PubMed]
34. Yu, F.; Fei, X.; He, Y.; Li, H. Poly(lactic acid)-based composite film reinforced with acetylated cellulose nanocrystals and ZnO nanoparticles for active food packaging. *Int. J. Biol. Macromol.* **2021**, *186*, 770–779. [CrossRef] [PubMed]
35. dos Santos, A.D.A.; Matos, L.C.; Mendonça, M.C.; do Lago, R.C.; dos Santos Muguet, M.C.; Damásio, R.A.P.; Ponzecchi, A.; Soares, J.R.; Sanadi, A.R.; Tonoli, G.H.D. Evaluation of paper coated with cationic starch and carnauba wax mixtures regarding barrier properties. *Ind. Crops Prod.* **2023**, *203*, 117177. [CrossRef]
36. Leung, Y.H.; Chan, C.M.N.; Ng, A.M.C.; Chan, H.T.; Chiang, M.W.L.; Djurišić, A.B.; Ng, Y.H.; Jim, W.Y.; Guo, M.Y.; Leung, F.C.C.; et al. Antibacterial activity of ZnO nanoparticles with a modified surface under ambient illumination. *Nanotechnology* **2012**, *23*, 475703. [CrossRef]
37. Reddy, K.M.; Feris, K.; Bell, J.; Wingett, D.G.; Hanley, C.; Punnoose, A. Selective toxicity of zinc oxide nanoparticles to prokaryotic and eukaryotic systems. *Appl. Phys. Lett.* **2007**, *90*, 213902. [CrossRef]
38. Pasquet, J.; Chevalier, Y.; Couval, E.; Bouvier, D.; Noizet, G.; Morlière, C.; Bolzinger, M.A. Antimicrobial activity of zinc oxide particles on five micro-organisms of the challenge tests related to their physicochemical properties. *Int. J. Pharm.* **2014**, *460*, 92–100. [CrossRef]
39. Stassinopoulos, A.; Tsagarakis, E.D.; Das, R.N.; Giannelis, E.P.; Anastasiadis, S.H.; Anglos, D. Laser-like emission from highly scattering ZnO nanoparticle films. *AIP Conf. Proc.* **2014**, *1172*, 44–48. [CrossRef]
40. MacCuspie, R.I. Colloidal stability of silver nanoparticles in biologically relevant conditions. *J. Nanopart. Res.* **2011**, *13*, 2893–2908. [CrossRef]
41. Alam, F.; Balani, K. Role of silver/zinc oxide in affecting de-adhesion strength of Staphylococcus aureus on polymer biocomposites. *J. Mater. Sci. Eng. C* **2017**, *75*, 1106–1114. [CrossRef]
42. Obeng, E.; Feng, J.; Wang, D.; Zheng, D.; Xiang, B.; Shen, J. Multifunctional phototheranostic agent ZnO@Ag for anti-infection through photothermal/photodynamic therapy. *Front. Chem.* **2022**, *10*, 1054739. [CrossRef]
43. Lomelí-Marroquín, D.; Cruz, M.D.; Nieto-Argüello, A.; Vernet Crua, A.; Chen, J.; Torres-Castro, A.; Webster, T.J.; Cholula-Díaz, J.L. Starch-mediated synthesis of mono- and bimetallic silver/gold nanoparticles as antimicrobial and anticancer agents. *Int. J. Nanomedicine* **2019**, *14*, 2171–2190. [CrossRef] [PubMed]
44. He, Y.; Ingudam, S.; Reed, S.; Gehring, A.; Strobaugh, T.P., Jr.; Irwin, P. Study on the mechanism of antibacterial action of magnesium oxide nanoparticles against foodborne pathogens. *Nanobiotechnology* **2016**, *14*, 54. [CrossRef] [PubMed]
45. Nundy, S.; Ghosh, A.; Mallick, T.K. Hydrophilic and superhydrophilic self-cleaning coatings by morphologically varying ZnO microstructures for photovoltaic and glazing applications. *ACS Omega* **2020**, *5*, 1033–1039. [CrossRef] [PubMed]
46. Myint, M.T.Z.; Kumar, N.S.; Hornyak, G.L.; Dutta, J. Hydrophobic/hydrophilic switching on zinc oxide micro-textured surface. *Appl. Surf. Sci.* **2013**, *264*, 344–348. [CrossRef]

Disclaimer/Publisher's Note: The statements, opinions and data contained in all publications are solely those of the individual author(s) and contributor(s) and not of MDPI and/or the editor(s). MDPI and/or the editor(s) disclaim responsibility for any injury to people or property resulting from any ideas, methods, instructions or products referred to in the content.